



HAL
open science

Swarming of micron-sized hematite cubes in a rotating magnetic field – Experiments

Oksana Petrichenko, Guntars Kitenbergs, Martins Brics, Emmanuelle Dubois, Régine Perzynski, Andrejs Cēbers

► **To cite this version:**

Oksana Petrichenko, Guntars Kitenbergs, Martins Brics, Emmanuelle Dubois, Régine Perzynski, et al.. Swarming of micron-sized hematite cubes in a rotating magnetic field – Experiments. Journal of Magnetism and Magnetic Materials, 2020, 500, pp.166404. 10.1016/j.jmmm.2020.166404 . hal-03039012

HAL Id: hal-03039012

<https://hal.science/hal-03039012>

Submitted on 3 Dec 2020

HAL is a multi-disciplinary open access archive for the deposit and dissemination of scientific research documents, whether they are published or not. The documents may come from teaching and research institutions in France or abroad, or from public or private research centers.

L'archive ouverte pluridisciplinaire **HAL**, est destinée au dépôt et à la diffusion de documents scientifiques de niveau recherche, publiés ou non, émanant des établissements d'enseignement et de recherche français ou étrangers, des laboratoires publics ou privés.

Swarming of micron-sized hematite cubes in a rotating magnetic field - Experiments

Oksana Petrichenko^{a,*}, Guntars Kitenbergs^a, Martins Brics^a, Emmanuelle Dubois^b, Régine Perzynski^b and Andrejs Cēbers^a

^aMMML lab, University of Latvia, Jelgavas 3, Riga, LV-1004, Latvia

^bPHENIX lab, Sorbonne University, CNRS, 4 place Jussieu, Paris, 75252, France

ARTICLE INFO

Keywords:
swarms
hematite cubes
magnetic particles
rotating field

ABSTRACT

Energy input by under-field rotation of particles drives the systems to emergent non-equilibrium states. Here we investigate the suspension of rotating magnetic cubes. Micron-sized hematite cubes are synthesized and observed microscopically. When exposed to a rotating magnetic field, they form rotating swarms that interact with each other like liquid droplets. We describe the swarming behaviour and its limits and characterize the swarm size and angular velocity dependence on the magnetic field strength and frequency. A quantitative agreement with a theoretical model is found for the angular velocity of swarms as a function of the field frequency.

1. Introduction

Ensembles of rotating particles, the so-called spinners, recently have obtained growing interest as a particular case of the active matter [1]. The benchmark case of these systems is ensembles of magnetic particles, whose rotation may be caused by a rotating field [2, 3] or arise by breaking the chirality, for example in the case of phototactic hematite particles [4].

The research in this field now fast developing and very interesting new features are found. Here we mention some of them. In [5, 6] it is shown that particle spinning and vortex may be caused also by CW/CCW symmetry breaking in a unidirectional AC field. Fingering instabilities of ensembles of rolling particles under the action of a rotating field are explored in [7]. Vortices formation and their self-organization in suspension of superparamagnetic beads under the action of a precessing field is described in [8]. The role of hydrodynamic interactions in systems of rolling particles is elucidated in [9].

Rotating crystals of biological origin were observed in [10], where fast moving rotating bacteria accumulated on the cell walls due to the hydrodynamic interaction formed collectively rotating ensemble. Recently a model considering the lubrication forces between close rotating particles has been introduced [11]. It predict characteristic features of an aggregate of rotating particles – edge effect in ensembles of rotating particles, stick-slip motion, rationalized by the Frenkel–Kontorova like model.

The article begins with a materials and methods section, which includes the description of hematite cube synthesis, size and magnetic property characterization, microscopy observation methods and subsequent image processing tools. The next section depicts observation of the swarm formation in a qualitative manner. Further we focus on characterizing the swarm angular velocity both qualitatively and quantitatively. In section 3 we use a theoretical model from Belovs

et al. [11] to explain the peculiarities of hematite particles swarming in the rotating field by comparing it to experimental data. We finish by discussing the differences and drawing conclusions.

2. Materials and methods

2.1. Synthesis

The synthesis of hematite cubic particles is based on the gel-sol method of Sugimoto *et al.* [12, 13].

Sodium hydroxide solution in water (5.4 M) is gradually added to an iron chloride aqueous solution (2.0 M). During the mixing process, the solutions are stirred and the temperature increased till 75°C. It is important to note that the salt of the iron chloride should be crystallohydrate ($\text{FeCl}_3 \cdot 6\text{H}_2\text{O}$). Finally, the mixture is hermetically sealed and left in an oven at 100°C for 7 days. The formation of cubic (or pseudo-cubic) hematite proceeds by transformations of the iron oxide ($\text{Fe}(\text{OH})_3$) through akaganeite ($\beta\text{-FeOOH}$) to hematite. In such a way, a precursor, which includes both micron sized particles and nanoparticles of hematite, is obtained [13]. Washing (performed by ultrasonication and centrifugation) is the last step to obtain the micron sized hematite particles, which are of interest in this study. Finally, the hematite particles are functionalized with sodium dodecylsulfate (SDS). The pH of the resulting solution is adjusted by a tetramethylammonium hydroxide solution to 8.5–9.5 values. This procedure prevents hematite particles from irreversible sticking on the glass surface, induced by attractive van der Waals interactions [14].

2.2. Characterization

The synthesized cubic-shape hematite particles are characterized with microscopy techniques to investigate their size. For that the hematite particles are magnetically stirred in a freshly prepared solution of SDS in water, followed by pH adjustment (8.5 – 9.5).

Electron microscopy measurements are made with a dried sample of the hematite suspension, using a scanning electron

*Corresponding author, E-mail: oksana.petrichenko@lu.lv

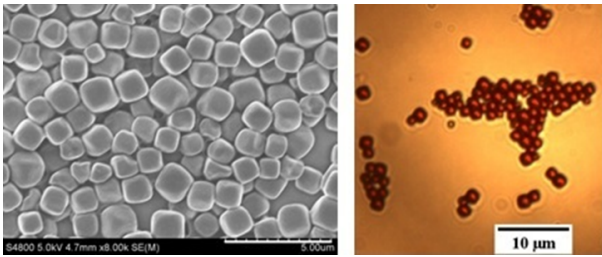


Figure 1: Images of hematite particles obtained by (a) scanning electron microscopy and (b) optical microscopy. Cubic-shape particles have a mean edge length $a \approx 1.6 \pm 0.3 \mu\text{m}$.

microscope Hitachi S4800 at 5.0 kV and $2000\times$ magnification. For optical microscopy a capillary of $100 \mu\text{m}$ thickness and 2 mm width (VitroCom VitrotubesTM) is then filled with the suspension of cubes via capillary forces and sealed with paraffin. It is imaged with $100\times$ magnification. As seen in images of Fig.1, obtained by both techniques, the resulting particles have a cubic shape with a similar edge length $a = 1.6 \pm 0.3 \mu\text{m}$. In addition, when observed with an optical microscope, the cubes tend to form fluctuating aggregates, where the attraction is due to magnetic and van der Waals interactions and fluctuations come from Brownian motion.

Magnetic properties for a dried sample are determined by a vibrating sample magnetometer (Lake Shore Cryotronics, Inc., 7400 VSM). The magnetization curve (not shown here) indicates a clear hysteresis and notable coercivity ($H_c = 3.5 \text{ kG}$). Remanent magnetization is around $\sigma = 0.2 \text{ emu/g}$, which corresponds to the particle magnetization $M = 1.1 \text{ G}$.

2.3. Video microscopy

Experiments were done in two laboratories in Riga and Paris. The system in Riga is based on an inverted microscope Leica DMI3000B. A custom made coil device with 2 perpendicular pairs of coils provide a homogeneous field in the plane of observation. The coils are run by Kepco BOP 20-10M power supplies, which are controlled with a NI DAQ card via a LabView program. Sinusoidal signals with a 90° phase difference creates a homogeneous rotating field at the field of observation up to 1 kHz. The process is filmed in a brightfield mode by a color camera Leica DFC310 FX (1.4MP). Using $100\times$ objective with oil immersion and $0.70\times$ camera mount provides a $130 \times 95 \mu\text{m}^2$ field of view.

The system in Paris is very similar and is described in [15]. In comparison, it uses $40\times$ objective, but allows to make recordings with a synchronized magnetic field up to 60 Oe and a frame rate up to 60 fps.

2.4. Image analysis

The experimental images are analyzed both qualitatively and quantitatively. For qualitative analysis, the ImageJ program is used to analyze individual cubes, observe aggregates and swarm formation and approximate sizes.

For quantitative analysis, a MatLab code for swarm angular velocity and size determination is developed. First, to find the an aggregate or swarm, each image is inverted

and thresholded. Using the intensity information only coming from pixels of particle aggregates allows to remove the background. Then the center of the aggregate is found by calculating the center of mass. The aggregate size is found by averaging intensities I in polar coordinates, which are normalized by the total aggregate intensity. As the aggregate radius R we take the size at initial state. The swarm angular velocity is found by cross-correlation of two images. To exclude the magnetic field direction influence (swarms tend to consist of short chains of cubes that rotate with the field), images with the same field direction are used. **Such images pairs are found using integer factorization of image recording and magnetic field frequencies.** The second image is rotated around the centre of mass by multiple angles and cross-correlated with the first image. Both images are normalized, therefore, the correlation peak value can be used to identify the angle between swarms in the two images. Dividing it by the time between images, one finds the swarm angular velocity Ω . It is averaged over the set of images for each frequency, obtaining the mean value and its error.

3. Results and discussion

When a suspension of hematite cubes is exposed to an in-plane rotating magnetic field, we observe a spontaneous swarming (see Fig.2). We start our experiment with a low and constant field frequency ($f = 0.5 \text{ Hz}$), while gradually increasing the magnetic field strength. At $H = 1.65 \text{ Oe}$ (Fig.2 (a)) hematite particles form single and double chains, that rotate around their axes and form swarm-like aggregates. An increase of field ($H = 3.30 - 9.90 \text{ Oe}$, (Fig.2 (b)–(c)) enhances swarming and we observe bigger elongated swarms which consist of multiple rotating chains. The longer semi-axis of the observed swarms reaches $75 \mu\text{m}$. By further increase of the field $H = 13.2 - 23.1 \text{ Oe}$ (Fig.2 (d)–(e)) the swarm formation continues, however, their further increase in size is limited by the number of surrounding particles. Cohesion forces responsible for swarm formation imply that swarms behave as liquid droplets. When they come close enough, swarms merge into one, as shown in Fig.3.

We then continue the experiment with increasing frequency, whereas magnetic field remains constant at $H = 23.1 \text{ Oe}$. Characteristic images are given in Fig.2 (f)–(j). Increasing the frequency up to 2.5 Hz induces a structural change in the aggregate–swarm behavior. The previously observed chains have split in individual cubes and dimers and the swarm shape becomes more regular (Fig.2(g)). Further increase of the frequency to $f = 10 \text{ Hz}$ transforms the swarms to more compact and circular shapes. Some individual cubes escape the swarms, but then return to them, if they come close enough (Fig.2(h)). Increasing frequency even more ($f \geq 50 \text{ Hz}$) induces a disintegration of the swarms, as can be seen in Fig.2 (i–j).

It should be noted that we have not observed a swarm formation by hematite particles with peanut or ellipsoidal shapes. Swarming of the particles with the peanut shape is observed in [16].

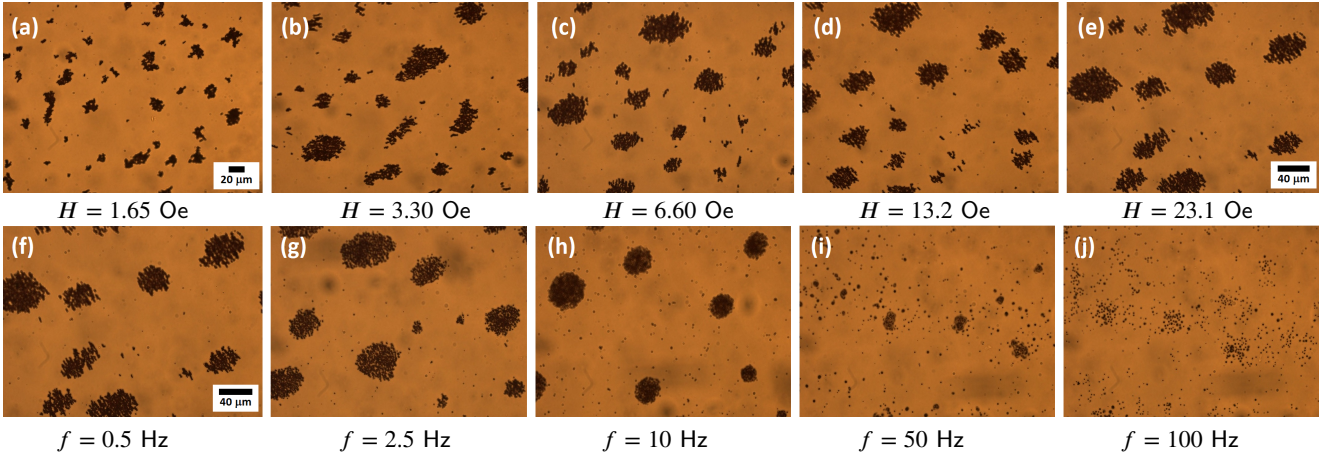


Figure 2: Swarming of hematite cubes under a rotating magnetic field. The first row (a)–(e) shows swarm development with the increasing magnetic field strength at the constant frequency $f = 0.5$ Hz. The second row (f)–(j) shows a change in swarm behavior with an increasing frequency at the constant field $H = 23.0$ Oe.

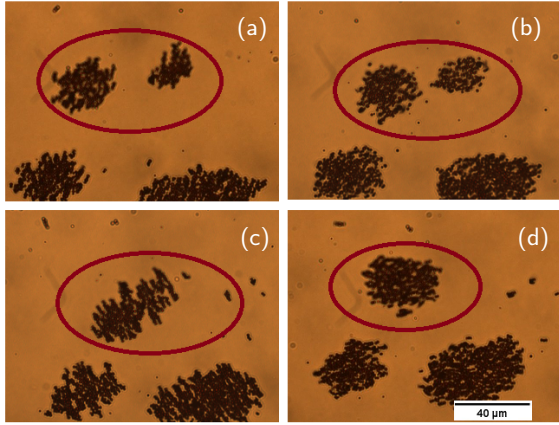


Figure 3: Fusion of two swarms at $H \approx 20$ Oe and $f \approx 0.6$ Hz. (a) $t = 0$ s, (b) $t = 164$ s (2.7 min), (c) $t = 192$ s (3.2 min), (d) $t = 295$ s (4.9 min). Scale bar is $40 \mu\text{m}$.

As mentioned in the introduction, recent theoretical results on rotating field driven ensembles [11] motivate us to investigate the swarm rotation experimentally in more detail. We perform a detailed study of several swarms using the setup in Paris, where the magnetic field direction is known for each image. Two rotating field amplitudes are exploited (33 Oe and 58 Oe), with varying frequencies from 0.01 Hz to 50.0 Hz. Characteristic images can be seen in Fig.4. They have been selected to show the rotation behavior. For each frequency series of three images are chosen. The first series corresponds to a magnetic field direction as close as possible to the upwards direction. The second corresponds to a field direction at 120° with respect to the first one. The third one corresponds to the image with a field direction pointing in the same direction as in the first image.

The rotational behavior of aggregates–swarms as a function of the frequency f at a given field can be split in 3 regimes (see Fig.4). This behaviour is also pronounced in the aggregate–swarm size, which is characterized in Fig.5.

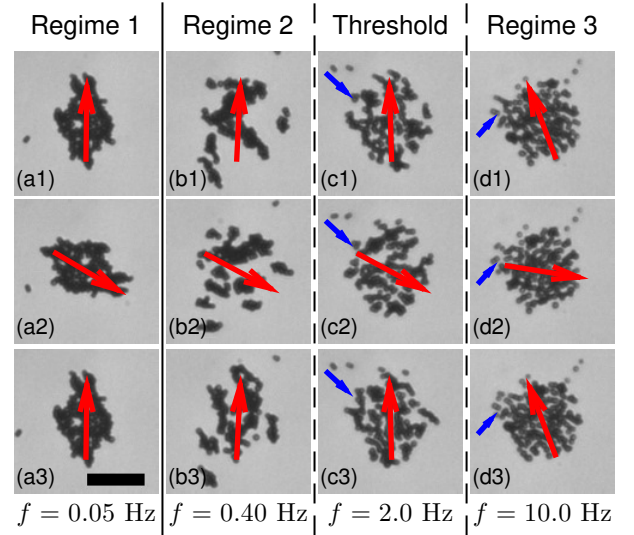


Figure 4: Aggregate rotation dynamics dependence on the field frequency can be split in 3 regimes: single aggregate, rotates with the field (a), multiple aggregates recombining, rotating with the field (b) and single cubes and dimers rotating with the field and forming a rotating swarm (d). (c) marks the threshold between regimes 2 and 3. The large red arrow indicates the direction of the field. The small blue arrow marks a reference point to see particle displacement. Images are taken for a swarm with the initial radius $R = 10 \mu\text{m}$ at $H = 33$ Oe at the following times: for (a) $t_{(a1)} = 0.0$ s, $t_{(a2)} = 6.7$ s, $t_{(a3)} = 20.0$ s; for (b) $t_{(b1)} = 0.0$ s, $t_{(b2)} = 0.8$ s, $t_{(b3)} = 10.0$ s; for (c) $t_{(c1)} = 0.0$ s, $t_{(c2)} = 0.17$ s, $t_{(c3)} = 0.5$ s and for (d) $t_{(d1)} = 0.0$ s, $t_{(d2)} = 0.03$ s, $t_{(d3)} = 0.20$ s. Scale bar is $20 \mu\text{m}$.

Regime 1: If the magnetic field frequency is very low ($f < 0.1$ Hz), cubes form an aggregate that rotates as a solid body with the field. For example, see Fig.4(a) and a supplementary video S1. As the cubes are almost close packed in the aggregate, the radius is smallest (blue diamonds in Fig.5, $R \approx 10 \mu\text{m}$).

Regime 2: Increase of frequency splits the large aggregate

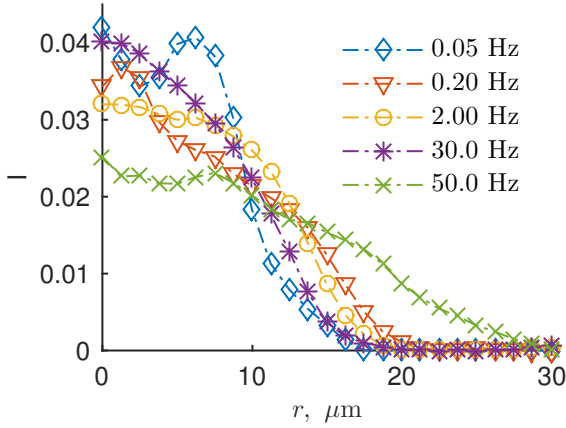


Figure 5: Characterization of the aggregate size by the distribution of the intensity I dependence on the radial distance r at various field frequencies f . The initial radius $R \approx 10 \mu\text{m}$, the magnetic field is $H = 33 \text{ Oe}$.

gate in several smaller aggregates that collide with each other and rotate with the field. An example can be seen in Fig.4 (b) and supplementary video S2. The transition to this second regime happens already at around $f=0.10 \text{ Hz}$. Initially this spreads the aggregate and slightly increases its size (red triangles in Fig.5). A further frequency increase reduces the size of hematite aggregates in the aggregate, which rotate closer to each other, slightly decreasing the aggregate size (orange circles in Fig.5), up to around $f = 2.0 \text{ Hz}$ only single cubes or dimers can be observed. This regime contains the transition from a single aggregate (Regime 1) to a swarm (Regime 3).

Regime 3: Swarms (aggregates that consist of rotating single cubes or dimers) have a clearly circular shape, as can be seen in Fig.4 (c) & (d) and supplementary video S3. In addition, increase of the field frequency enables a faster rotation of the swarm. This keeps reducing the size (violet asterisks in Fig.5), almost to the average size of the large aggregate in Regime 1. **The transition from Regime 2 to 3 (indicated in Fig.4 (c) as threshold) appears to happen stepwise, probably due to the polydispersity of magnetic cubes.**

If the field frequency is increased even further ($f \approx 50 \text{ Hz}$), the swarms disassemble. This is clearly visible by the size increase (green crosses in Fig.5).

Further we analyze the swarm rotation quantitatively via the method described in section 2.4. Characterization of swarm rotation is only reasonable for the third regime. In the first regime ($f < 0.2 \text{ Hz}$) the particle aggregate rotates as a whole (solid rotation) and does not behave like a swarm of multiple particles. In the second regime ($0.2 < f < 2.0 \text{ Hz}$) several smaller rotating aggregates collide and reassemble in various combinations, making it impossible to define a collective angular velocity.

For the third regime the rotation of many individual particle induces a global rotation of the swarm. The swarm angular velocity Ω is presented in Fig.6 as a function of the field frequency f for swarms of different radii R at two dif-

ferent field strengths H . For frequencies larger than $f = 2.0 \text{ Hz}$, the swarm angular velocity first increases linearly. It is important to note that at this stage the swarm rotation frequency is ≈ 30 times smaller than the magnetic field frequency. When a critical frequency $f_c = 20..30 \text{ Hz}$ is reached, the swarm rotation slows down. At $f = 40..50 \text{ Hz}$ the angular velocity Ω goes quickly to zero, as the swarm starts to disassemble and individual particles move far away from each other.

Increase in magnetic field strength H increases the critical frequency f_c and allows to reach higher swarm angular velocities (green asterisks and blue diamonds in Fig.6), whereas swarms with a larger initial radius R rotate slower (orange crosses vs. violet circles in Fig.6). To have a more quantitative view, further measurements are necessary.

The data obtained for the angular velocity of swarm Ω as a function of the magnetic field frequency f (particle rotation frequency) reasonably well agree with the relation derived from the balance of lubrication forces at the edge of the swarm and friction near a solid wall in [11]

$$\frac{\tau\Omega}{F_d} = \frac{\pi}{\varphi_d} \frac{1}{(R/d)^2}, \quad (1)$$

where $\tau = d/(3m^2/2d^4\zeta)$ is a characteristic timescale, $F_d = \frac{1}{5} \ln(d/\delta) \frac{2\pi\eta 2\pi f d^6}{3m^2}$ is the driving force, d is the size of a particle, here assimilated to the cube edge size a , m is its magnetic moment, δ is the distance between surfaces of particles and φ_d is the area fraction of particles. We can estimate the hydrodynamic drag coefficient near solid wall as $\zeta = 3\pi\eta d \ln(d/\delta)$ and instead of π/φ_d take the value 5.6, which is more precise and obtained numerically in [11]. As a result, we get

$$\frac{\Omega}{f} = \frac{11.2\pi}{15} \frac{1}{(R/d)^2}. \quad (2)$$

For a swarm with the radius $R = 7.0 \mu\text{m}$, taking the particle size $d = a = 1.6 \mu\text{m}$, gives $\Omega/f = 0.17$, which is very close to the experimental data, as indicated by red dotted line in Fig.6. The dash-dotted black line shows a model prediction for a swarm of $R = 10 \mu\text{m}$, whereas the solid black line shows prediction for a swarm of $R = 5 \mu\text{m}$. Using $d = a = 1.6 \mu\text{m}$, the uncertainty of the measurement $\pm 0.3 \mu\text{m}$ affects the model prediction considerably. This is displayed in Fig.6 via gray areas, which correspond to the black lines. Nevertheless, we can see that the linear part of our measurements fits well these limits.

4. Conclusions

Swarming of hematite cubes in the rotating field is investigated experimentally. It is shown that in the intermediate range of frequency of the rotating field the swarm consists mainly of single rotating particles which drive the rotation of swarms with angular velocities smaller by an order of magnitude than the angular velocity of the field. The angular velocity of the swarm determined from the cross correlation

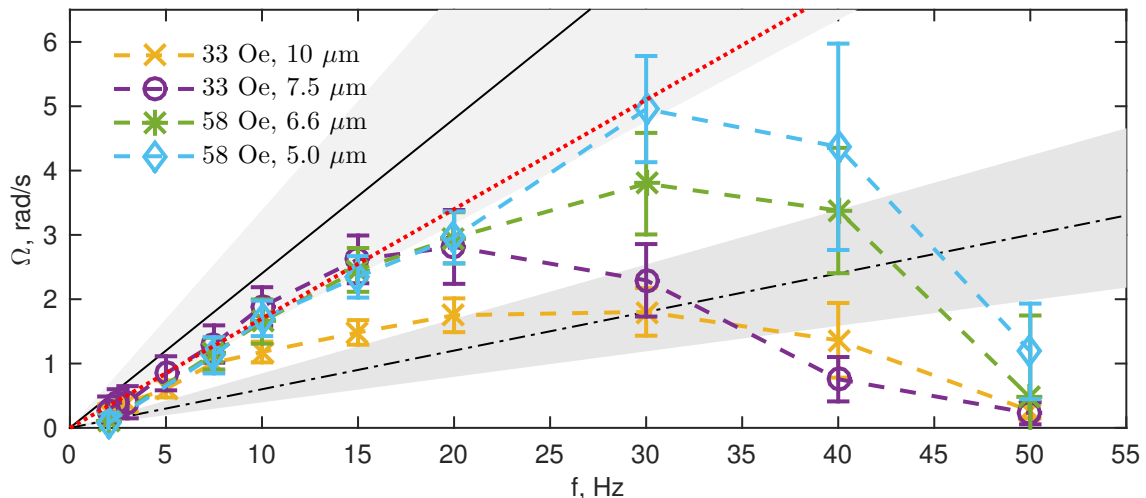


Figure 6: The swarm angular velocity Ω as a function of the field frequency f for four swarms of different sizes and magnetic fields, as indicated in the legend. The red dotted line shows a model prediction for $R/d = 7.0/1.6$. The black dash-dotted line for $R/d = 10/1.6$, the solid black line for $R/d = 5/1.6$. Gray areas indicate corresponding uncertainties to black lines, which come from the particle size distribution.

analysis of images reasonably well corresponds to the theoretical relation with respect to the field frequency and swarm size. Due to the action of cohesion forces, swarms behave like liquid droplets – two swarms, if close enough, merge similarly to two liquid droplets. At higher frequencies, when single particles do not follow anymore the rotating field, the swarms break.

Aknowledgements

Authors are very thankful to P.Tierno and H.Massana-Cid from the University of Barcelona for the instructions on hematite synthesis. Authors also thank colleagues from the University of Latvia – M.M.Maiov from the Institute of Physics for magnetic measurements and K.Buks from the Institute of Chemical Physics for SEM images of particles.

O.P. acknowledges support from PostDocLatvia grant No. 1.1.1.2/VIAA/1/16/018, G.K. from PostDocLatvia grant No. 1.1.1.2/VIAA/1/16/197 and M.B. and A.C. from M.era-net project FMF No.1.1.1.5./ERANET/18/04. All authors are thankful to the French-Latvian bilateral program Osmose project FluMaMi (n°40033SJ; LV-FR/2019/5).

Appendix A. Supplementary videos

Supplementary videos associated with this article can be found in the online version at ...

References

- [1] Y. Fily, A. Baskaran, M. C. Marchetti, Cooperative self-propulsion of active and passive rotors, *Soft Matter* 8 (2012) 3002–3009.
- [2] J. Yan, S. C. Bae, S. Granick, Rotating crystals of magnetic janus colloids, *Soft Matter* 11 (2015) 147–153.
- [3] V. Soni, E. Bililign, S. Magkiriadou, S. Sacanna, D. Bartolo, M. J. Shelley, W. T. M. Irvine, The free surface of a colloidal chiral fluid: waves and instabilities from odd stress and hall viscosity, 2018. arXiv:1812.09990.
- [4] A. Aubret, M. Youssef, S. Sacanna, J. Palacci, Targeted assembly and synchronization of self-spinning microgears, *Nature Physics* 14 (2018) 1114–1118.
- [5] G. Kokot, S. Das, R. G. Winkler, G. Gompper, I. S. Aranson, A. Snezhko, Active turbulence in a gas of self-assembled spinners, *Proceedings of the National Academy of Sciences* 114 (2017) 12870–12875.
- [6] A. Kaiser, A. Snezhko, I. S. Aranson, Flocking ferromagnetic colloids, *Science Advances* 3 (2017).
- [7] M. Driscoll, B. Delmotte, M. Youssef, S. Sacanna, A. Donev, P. Chaikin, Unstable fronts and motile structures formed by micro-rollers, *Nature Physics* 13 (2017) 375–379.
- [8] T. Mohorič, G. Kokot, N. Osterman, A. Snezhko, A. Vilfan, D. Babič, J. Dobnikar, Dynamic assembly of magnetic colloidal vortices, *Langmuir* 32 (2016) 5094–5101. PMID: 27128501.
- [9] F. Martinez-Pedrero, E. Navarro-Argemí, A. Ortiz-Ambriz, I. Pagonabarraga, P. Tierno, Emergent hydrodynamic bound states between magnetically powered micropropellers, *Science Advances* 4 (2018).
- [10] A. P. Petroff, X.-L. Wu, A. Libchaber, Fast-moving bacteria self-organize into active two-dimensional crystals of rotating cells, *Phys. Rev. Lett.* 114 (2015) 158102.
- [11] M. Belovs, M. Bricis, A. Cēbers, Rotating-field-driven ensembles of magnetic particles, *Phys. Rev. E* 99 (2019) 042605.
- [12] A. Muramatsu, S. Ichikawa, T. Sugimoto, Controlled formation of ultrafine nickel particles on well-defined hematite particles, *Colloids and Surfaces A: Physicochemical and Engineering Aspects* 82 (1994) 29 – 35.
- [13] T. Sugimoto, M. M. Khan, A. Muramatsu, Preparation of monodisperse peanut-type α -Fe₂O₃ particles from condensed ferric hydroxide gel, *Colloids and Surfaces A: Physicochemical and Engineering Aspects* 70 (1993) 167 – 169.
- [14] H. Massana-Cid, F. Martinez-Pedrero, E. Navarro-Argemí, I. Pagonabarraga, P. Tierno, Propulsion and hydrodynamic particle transport of magnetically twisted colloidal ribbons, *New Journal of Physics* 19 (2017) 103031.
- [15] J. Erdmanis, G. Kitenbergs, R. Perzynski, A. Cēbers, Magnetic microdroplet in rotating field: numerical simulation and comparison with experiment, *Journal of Fluid Mechanics* 821 (2017) 266 – 295.
- [16] H. Xie, M. Sun, X. Fan, Z. Lin, W. Chen, L. Wang, L. Dong, Q. He, Reconfigurable magnetic microrobot swarm: Multimode transformation, locomotion, and manipulation, *Science Robotics* 4 (2019).